SIC BASED COMPOSITES FOR WEAR APPLICATIONS

A DISSERTATION

Submitted in partial fulfilment of the

Requirements for the award of the degree

Of

MASTER OF TECHNOLOGY

In

METALLURGICAL AND MATERIALS ENGINEERING

(With Specialization in Materials Engineering)

By

DEEPAK KUMAR

(Enrolment No: 16545007)

DEPARTMENT OF METALLURGICAL AND MATERIALS ENGINEERING

INDIAN INSTITUTE OF TECHNOLOGY ROORKEE

ROORKEE –247667 (INDIA)

May2018

Indian Institute of Technology Roorkee

Roorkee

CANDIDATE'S DECLARATION

I hereby declare and certify that the work which is being presented in the DISSERTATION entitled **"SIC BASED COMPOSITES FOR WEAR APPLICATIONS"** in partial fulfilment of the requirement for the award of the DEGREE OF MASTER OF TECHNOLOGY with specialization in MATERIALS ENGINEERING submitted in the Departmet of Metallurgical and Materials Engineering of the Indian Institute of Technology Roorkee, Roorkee is an authentic record of my own work carried out during the period from May 2017 to May 2018 under the supervision of DR. B.V. Manoj Kumar, Associate professor, Department of Metallurgical and Materials Engineering, Indian Institute of Technology Roorkee, Roorkee.

The matter presented in this thesis has not been submitted by me for the award of any other degree of this or any other Institute.

Dated: May 2018

Place: Roorkee (DEEPAK KUMAR)

CERTIFICATE

This is to certify that the above statement made by the candidate is correct to the best of my knowledge and belief.

DR. B.V. MANOJ KUMAR

Associate Professor,

MMED, IIT Roorkee

Roorkee- 247667 (India)

ACKNOWLEDGEMENT

I would like to express my gratitude and thanks to my guide Dr. B.V. Manoj Kumar, Assistant Professor, Metallurgical and Materials Engineering Department, Indian Institute of Technology Roorkee, for his valuable guidance, inspiration and generous help in carrying out this work. It would not have been possible to materialize the concepts in the area of **"SIC BASED COMPOSITES FOR WEAR APPLICATIONS"**, as without his proper guidance completing this project would have been a monumental task. Working under him was a privilege and an excellent chance to learn and grow, which I will cherish for the life time.

I wish to express my sincere thanks to Dr. Anjan Sil, Professor and Head of the Department ,Metallurgical and Materials Engineering Department, IIT ROORKEE, for his help to carry out this dissertation.

My heartfelt thanks goes to Mr. Yashpal Sharma and Mr. Nilesh V Dorkar, Research Scholar, MMED for their guidance and relentless support and help during the whole work and making me understand portion of work which I was unable to understand.

Special thanks goes to all the lab members and faculty for their help and kind co-operation throughout the course of my project work.

I would like to acknowledge my friends for their valuable information and help, and boosting my morale throughout the work.

Last but not the least, I would like to thank my parents for making me walk this earth and for all they did, after which everything else was possible.

ABSTRACT

The present work deals with the samples prepared with composition 0,5,10,35Vol.%BN in SiC with additive Y_2O_3 by Spark Plasma Sintering parameters to check the change in microstructure and the resulting changes that accompanies with the hardness and fracture toughness. The sintering parameters were changed to achieve a high dense material. The final SPS parameters were maximum temperature 1800℃. In all cases the holding time was kept at 5min at the final temperature. The heating rate was kept at 100℃/min for all samples. Load applied was 55MPa. SEM images reveal the formation of structure for the samples. SEM images of the fractured surfaces shows how the fracture is takes place and hoe the BN content will effect the type of fracture. Hardness and fracture toughness of the samples is 19.20±0.2 GPa max.for the SBN5 and 3.93Mpa-$m^{1/2}$ max. for SBN35. After that the dry sliding wear test shows that the wear track width is decrease with increase in BN content shows the severity of the wear and also the wear volume is decreases as the BN content is decreased. Fractures surfaces of the composites shows how the BN content will effect the transgranular fracture also there is pull-out of material takes place

Contents

List of figures

List of Tables

1.1 Silicon-Carbide/Boron-Nitride Composites

Silicon carbide (SiC) ceramics have long received attention due to their technological merits including their thermal and mechanical properties as well as wear and corrosion resistance [1–9]. Rigid SiC ceramics containing high percentage of thermal conductivity and chemical stability utilises various industrial applications such as mechanical seals, bearings, heat-sink plates,automobile parts,and protective walls for nuclear reactors.However,the brittlene ss of SiC materials is a major impediment for engineering applications, which also increases the difficulty of machining and cost. Also, SiC has low thermal shock resistance, which leads to a deterioration of its potential. There are several ways to improve these disadvantageous properties of SiC ceramics. Combining with other materials to form a hybrid structure can improve the fracture toughness and the thermal shock resistance of the ceramic materials. For adjusting the elastic modulus making porous materials with different porosity and composites by adding phases with low elastic modulus are the main approaches.Thus, one valid method for improving the disadvantageous properties of SiC ceramics is making a composite with ceramic reinforcement.Among ceramic reinforcement,hexagonalboron nitrid e (h-BN) is a candidate material as second phase, which has excellent thermal shock resistance and machinability [10,11]. Hexagonal BN (h-BN) is also known to have a high electrical resistivity as well as allow thermal expansion coefficient [10]. These properties of BN have led to its use in a variety of specialized areas including crucibles for molten metals and the sintering of nitride ceramics, break rings for horizontal continuous casting of steel and thermal protection tubes. One approach for tailoring properties is to combine the proper-ties of different materials. A new approach that has received less attention is the incorporation of h-BN in SiC without the use of sintering additives. The incorporation of h-BN in SiC can modify the electrical and mechanical properties of SiC ceramics, improve their thermal shock resistance, and impart machinability to SiC ceramics [12–14].

Objective of the thesis:

The major objectives of the thesis are as follows:

i. To prepare dense SiC-h-BN composites with varying h-BN content by optimum conditions of spark plasma sintering.
ii. To study microstructural and phase evolution of sintered composites.
iii. To evaluate mechanical properties of sintered composites.
iv. To understand wear behavior of SiC-h-BN composites as function of h-BN content and wear test parameters.

1.2 Structure of thesis

To investigate the above mentioned objectives, the thesis is structured as per the following:

Chapter-2 Literature review

A review of the published available literature in areas that are directly relevant to the present study is presented in this chapter2. It gives a deep insight into composition, microstructure, properties and processing techniques of SiC based composites.

Chapter-3 Experimental details

Details including powders used, compositions investigated, spark plasma sintering are explained. This is followed by details of density measurement, microstructural characterization, hardness, wear of composites.

Chapter-4 Results and Discussion

In this chapter, a discussion on major results obtained in preparation and characterization composite is provided, spark plasma sintering are discussed. This is followed by detailed discussion on microstructural characteristics, wear of composites.

Chapter-5 Conclusions and future scope

Important conclusions drawn from the present thesis work and future directions are suggested in this chapter.

2.1 SiC Ceramics

Silicon carbide is an important non-oxide ceramic which has diverse industrial applications. In fact, it has exclusive properties such as high hardness and strength, chemical and thermal stability, high melting point, oxidation resistance, high erosion resistance, etc. All of these qualities make SiC a perfect candidate for high power, high temperature electronic devices as well as abrasion and cutting applications. Quite a lot of works were reported on SiC synthesis since the manufacturing process initiated by Acheson in 1892. In this chapter, a brief summary is given for the different SiC crystal structures and the most common encountered polytypes will be cited. Emphasis is given on various fabrication routesvof SiC starting from the traditional Acheson process which led to a large extent into commercialization of silicon carbide. This process is based on a conventional carbothermal reduction method for the synthesis of SiC powders. Nevertheless, this process involves numerous steps, has an excessive demand for energy and provides rather poor quality materials. Several alternative methods have been previously reported for the SiC production. An overview of the most common used methods for SiC elaboration such as physical vapour deposition (PVT), chemical vapour deposition (CVD), sol-gel, liquid phase sintering (LPS) or mechanical alloying (MA) will be detailed. The resulting mechanical, structural and electrical properties of the fabricated SiC will be discussed as a function of the synthesis methods [15-18].

2.2 Chemical bonding and crystal Structure

The formation of SiC from the reaction between silicon and carbonvcan take place at temperatures below the melting point of silicon. There are numerous (~200) polytypes for SiC, but only a few are common. All of the structures may be visualized as being made up of a single basic unit, a layer of tetrahedral, in which each silicon atom is tetrahedrally bonded to four carbon atoms and each carbon atom is tetrahedrally bonded to four silicon atoms. The differences among the existing polytypes are the orientational sequences by which such layers of tetrahedra are stacked. Successive layers of tetrahedra may be stacked in only one of two ways or orientations but with many possible sequential combinations, each of which represent a different crystal polytype. A common system of nomenclature used to describe the different crystalline polytypes assigns a number corresponding to the number of layers in the unit cell

followed by a letter suffix designating the crystal symmetry; "C" for cubic, "H" for hexagonal and "R" for rhombohedral. The most common SiC polytypes are the 3C, 4H, 6H, 15R and 9T. The cubic 3C is commonly referred to as beta silicon carbide, β-SiC, which has the zinc blend structure, while all other polytypes are referred to as alpha silicon carbide, α-SiC. In general, α-SiC phase is mainly 6H, which is a wurtzite structure. Figure 1 shows an illustration of the two major crystal structures, zinc blend and wurtzite, exhibited by the two SiC phases. Phase transformation of SiC occurs from β-SiC to α-SiC upon heating. Undoped β-SiC transforms to 6H and 15R above 2000°C, with the 15R being a metastable phase that transforms to 6H. Doping β-SiC with boron lowers the transformation temperature and results in the formation of 4H polytype. On the other hand, doping with nitrogen prevents the formation of 4H and stabilizes the 6H. The β → α phase transformation is irreversible under ambient atmosphere. However, under pure nitrogen atmosphere, the transformation can be reversed and β-SiC phase can be stabilized up to 2500°C by applying a nitrogen pressure. Under atmospheric pressure, silicon carbide does not melt when heated to elevated temperatures rather, it sublimes and/or dissociates. In addition, incongruent melting of SiC was reported at 2829°C under >500 psi pressure of argon and is also possible when it is heated rapidly in an arc-image furnace at atmospheric pressure.

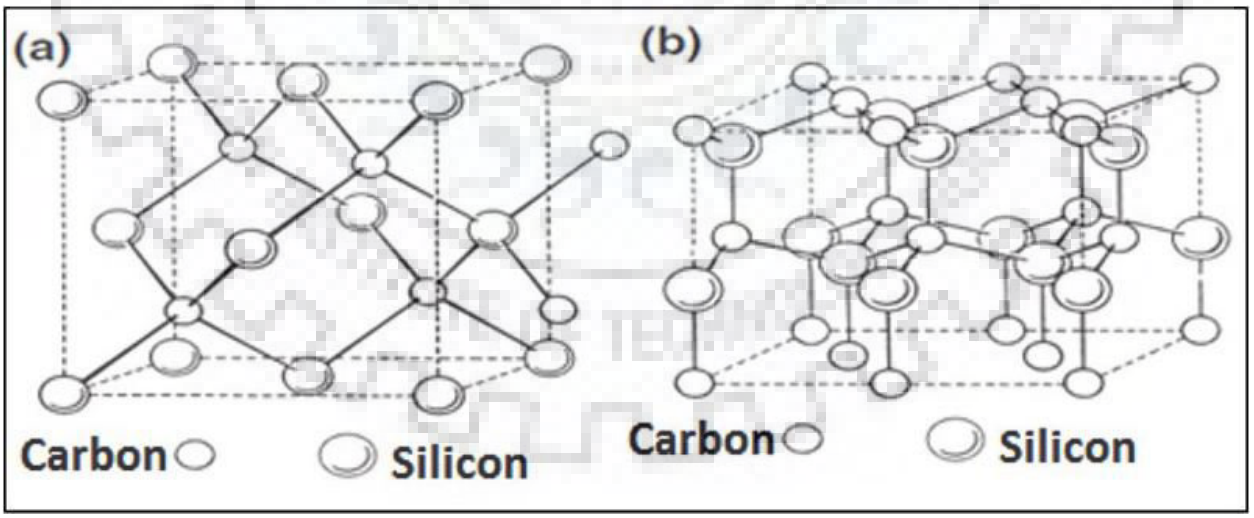

Fig.1 SiC Crystal Structures: (a) Zinc Blend Structure for β-SiC and (b) Wurtzite Structure α-SiC. (From:Kingery et al, "Introduction to Ceramics", 2nd., Wiley, New York, 1976, p. 63)

2.3 Properties of SiC

Silicon carbide is a candidate material forvhigh temperature structural applications because of its good mechanical properties, and excellent corrosion and oxidation resistance.Silicon carbide has been recognized as an important material with a wide range of industrial applications because of its good thermal conductivity, high mechanical strength, and oxidation and corrosion resistance. The various properties of Silicon Carbide are given in Table1:

Table1: Properties of Silicon Carbide Ceramics (ref17)

Physical	**Units**	**SI/Metric**
Density	g/cc	321
Hardness	Kg/mm^3	2800
Compressive Strength	MPa	3900
Elastic Modulus	GPa	416
Flexural Strength	MPa	550
Fracture Toughness	$MPam^{1/2}$	46
Poisson's ratio	-	0.14
Melting Point	°C	2780
Maximum Use Temperature	°C	1650
Thermal Conductivity	W/m-k	120
Coefficient of Thermal expansion	10^{-6}/ °C	4.0
Specific Heat	J/kg-k	750
Volume Resistivity	Ohm*cm	10^2-10^6

2.4 Applications of SiC

It is used in abrasives, refractories, ceramics, and numerous high-performance applications. The material can also be made an Electrical Conductor and has applications in Resistance Heating, Flame Igniters and Electronic Components. Structural and Wear applications are constantly developing.

2.4.1 As Abrasive

It is widely used as abrasive because of its hardness and low cost. It is used on grinders, energy powers and as abrasives material in water jet cutting and wear testing.

2.4.2 Ball bearings and seal ring

Silicon carbide is also used in ball bearings and seal rings due to is combination of favorable properties like high hardness, high elastic modulus and low density, low coefficient of thermal expansion, high chemical corrosion resistance etc.

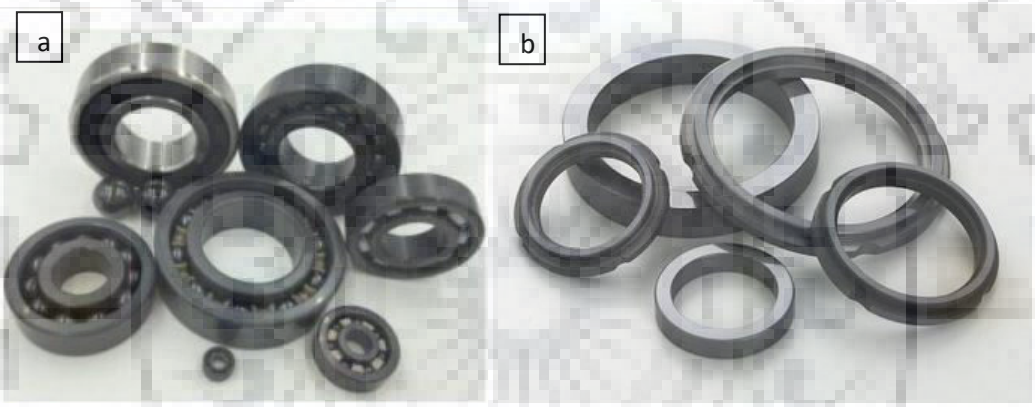

Fig2 (a) SiC ball bearings (b) SiC seal rings [19]

2.4.3 Cutting tool applications

Cutting tools usually must be hot-pressed to achieve full density and the necessary thermal-mechanical properties. Such toolsvare cost-effective for shaping difficult-to-machine metals such as steel and Ni-based superalloys forvturbines in aerospace applications. For the cutting tool application, one is generally interested in the following properties of the composite: fracture toughness, thermal conductivity, abrasive wear resistance, chemical inertness, and thermal shock resistance. During cutting steels with tools of Al_2O_3-SiC_w, damage is accompanied by whisker toughening mechanisms and reaction may occur between SiC. This generally limits cutting of ferrous materials to lower speeds.

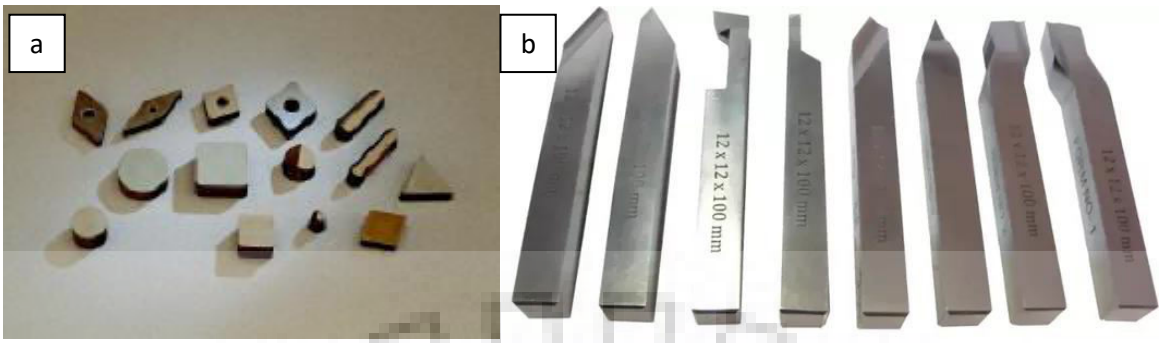

Fig. 3 (a) SiC based cutting Tool inserts (b) SiC based cutting tools [19]

2.4.4 For defence applications:

Silicon carbide has many applications in defence. Many components like proof vests. Cobham armour which is used to protect main battle tanks and dragon skin are prepared by silicon carbide.

Fig4 Bullet Proof Vests [19]

2.4.5 For automobile applications:

Silicon carbide is widely used in automobiles. Automobiles parts are like brakes and clutches plates and diesel filters.

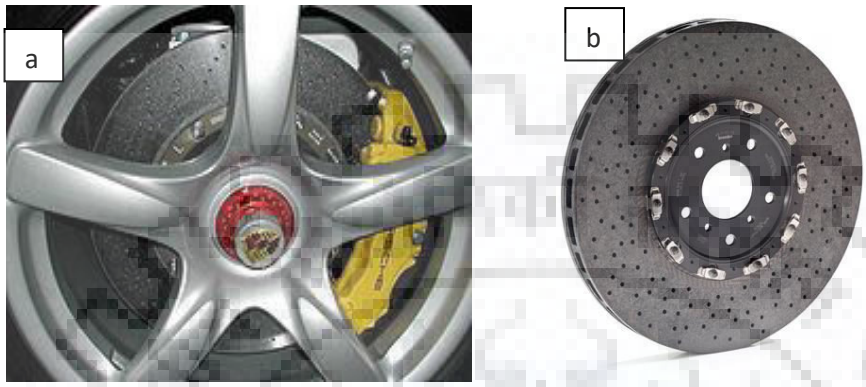

Fig5 (a) Disk brakes (b) Clutch Plates [18]

2.5 SiC ceramics and their composite

2.5.1 Effect of Alumina

Unlu et al reported the effect of alumina on the spark plasma sintering of SiC ceramics. SiC ceramics were prepared with the addition of alumina as sintering additive by spark plasma sintering at e different temperatures in the range of 1700-1800 ◦C applying two different pressures 40 and 80MPa under vacuum atmosphere.. The hardness and fracture toughness of the samples were evaluated by the Vickers indentation technique. Microstructure of spark plasma sintered SiC samplesvwere characterized by using scanning electron microscopyvtechnique.

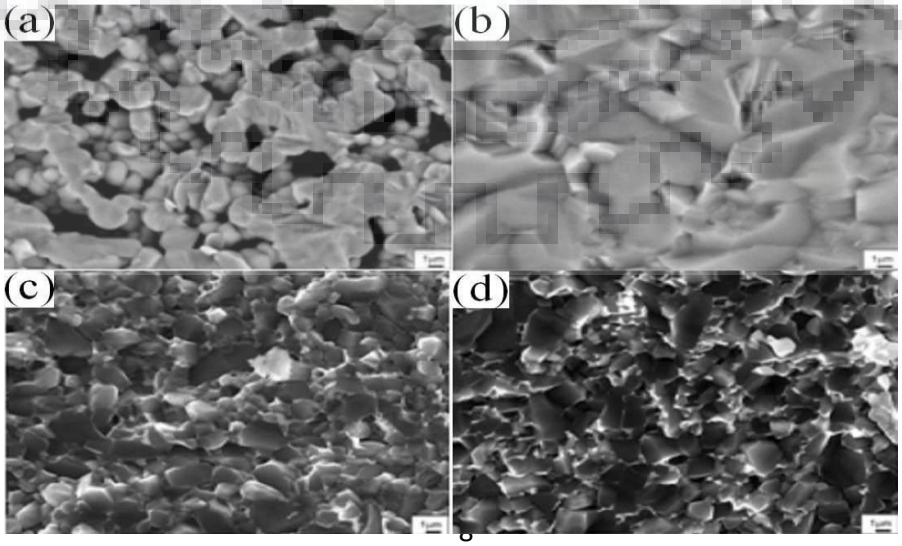

Fig.7. SEM images of fracture surfaces of SiC ceramics (a) at 1800 ◦C at 40 MPa, (b)1950 ◦C at 80 MPa, (c) SiC+5 vol.% Al2O3at 1800 ◦C under at 40 MPa, (d) SiC+5 vol.% Al2O3 at 1800 ◦C at 80 MPa

Table2 Relative density, Vickers hardness, fracture toughness of SiC ceramics with Al_2O_3

Samples	SPS parameters (°C, MPa, min.)	Relative density (%)	Vickers hardness (GPa)	Fracture Toughness (MPa*$m^{1/2}$)
SiC+5vol.%Al_2O_3	1700,40,5	97.7	26.4	4.6±0.2
	1800.40,5	97.8	26.9	5.8±0.5
	1700,80,5	97.5	26.2	5.7±0.2
	1800,80,5	98.3	28.9	5.9±0.2
Monolithic SiC	1800,80,5	87.2	10.2	-
	1950,80,5	99.7	31.9	3.6±0.3

2.5.4 SiC-BN composites

Seo et al. were studied SiC-BN composite which were fabricated by conventional hot-pressing from -SiC and h-BN powders with 2 vol.% Y_2 O_3 as a sintering additive. Electrical, mechanical, and thermal properties of SiC-BN composites were investigated as a function of the BN content in the starting materials. The addition of BN sup-pressed the grain growth of the SiC and triggered the β →α phase transformation of the SiC in SiC-BN composites. A minimum electrical resistivity of 3.7 × 10^{-2} _ cm was obtained for the SiC-4 vol.% BN composite (SBN4). This low electrical resistivity was ascribed to N-doping in the SiC lattice, which acts as a donor for supplying electrons to the conduction band. Typical values for the electrical conductivity, fracture toughness, flexural strength, and thermal conductivity of the SBN4 at room temperature were 27 $^{-1}$ cm^{-1} , 4.1 MPa $m^{1/2}$, 566 MPa, and 87 W/m K, respectively. The SiC-4 vol% BN composite can be electrical discharge machined to form complex shapes.

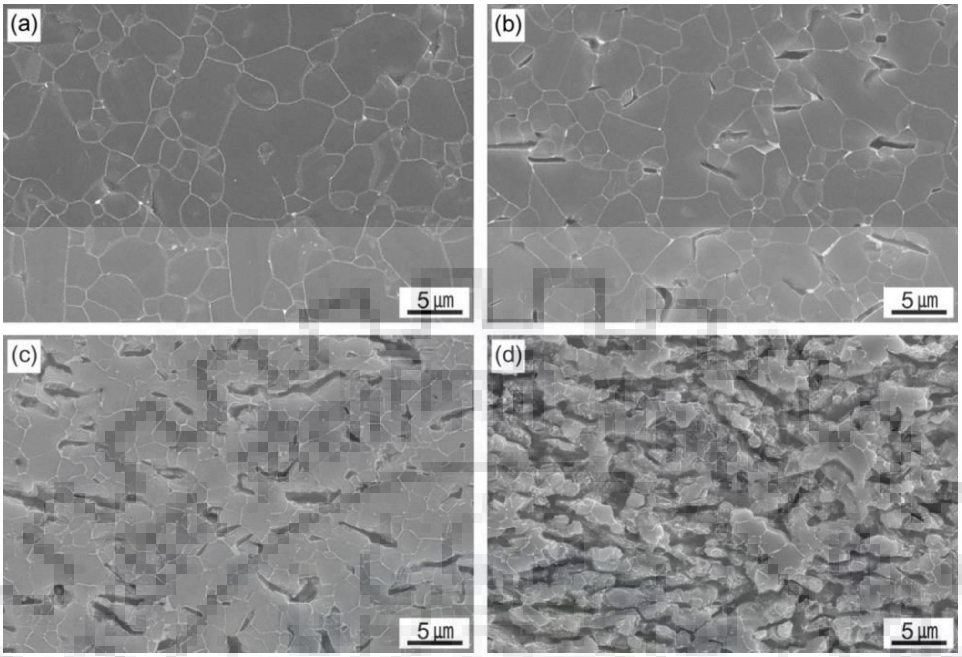

Fig. 9 Typical microstructures of monolithic SiC and SiC-BN composites sintered with 2 vol.% Y_2O_3 : (a) SBN0, (b) SBN4, (c) SBN10, and (d) SBN35

2.5.6 Effect of Y_2O_3-Al_2O_3Additive

Zhang et al. studied what happens when addition of Y_2O_3-Al_2O_3 additive during phase formation and in densification process of in situ of SiC composite has been enquired. The in situ reaction started at 1450°C when the addition of Y_2O_3-Al_2O_3 additivevis not there. However, when Y_2O_3-Al_2O_3 is there the reaction was very fast and finished after hot pressing at 1700°C. During, dense material with well-crystallized SiC and BN grains is obtained. Denitrification mechanism is also there during the occurence reaction process for both specimens with or without Y_2O_3-Al_2O_3 However denitrification takes place continuously at higher temperature 1700°C for the specimen without Y_2O_3-Al_2O_3 additive and results that there is in the nitrogen content. Results from this effect explained based the following mechanism during the Y_2O_3-Al_2O_3 additive makes Y-Al-Si-O liquid phase with Silicon oxide present in Si_3N_4 powder, promote or increase diffusion of the elements of the reactants.

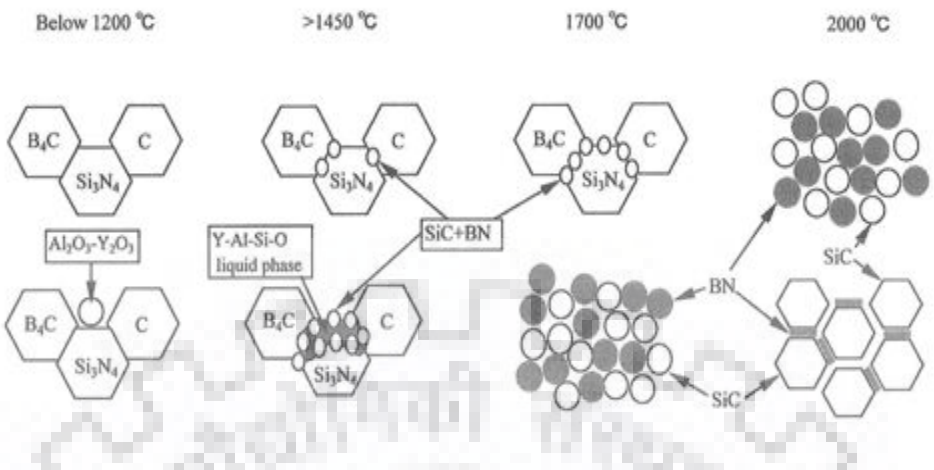

Fig10 Reaction sequences of the specimens with and without Y2O3-Al2O3 addition

2.6 Processing of composite

2.6.1 Milling of the powders

The SiC is mixed with BN(0,5,10,35vol.%) and Y_2O_3(2 wt%) were milled in a jar mill in a bottle containing tungsten carbide balls of 10 mm diameter and filled with toluene for 24 hours. The weight of the balls to the weight of the powder mixture to be milled is maintained in the ratio of 10:1. Moisture is removed from the powder by heating at 120°C for 3 hours and then sieved through a 45 μm sieve.

2.6.1 Sintering of powders

The conventional sintering method which requires high temperature holdings for long periods is unable to accomplish our requirement. So, some better processing route needs to be chosen. The various important sintering techniques are vacuum sintering (NS), hot isostatic pressing sintering (HIP), Microwave vacuum sintering (MVS), Spark plasma Sintering (SPS). The most advanced technique known till date for sintering ceramic powders is Spark Plasma Sintering (SPS). This method is adored for its unique advantages like low sintering temperature, low holding times, in-situ cleaning of oxide surfaces obtained cleaner materials with high consolidated densities. [20]. This method has been used in the present work, so it is discussed at detail in following paragraphs.

Before going into the details, it is pre-requisite to understand various concerns related to the sintering of ultrafine cermets. The major concern is of coarsening as the conventional sintering techniques subject sample to high temperatures and extended holding times which results in unacceptable grain growth. The driving force for sintering is reduction of surface energy, either by reducing total surface i.e. grain growth which is undesirable or by replacing solid-vapor interface with solid-solid interface, the latter leads to densification. But, there is a problem that both these phenomena compete with one-another [21-22].

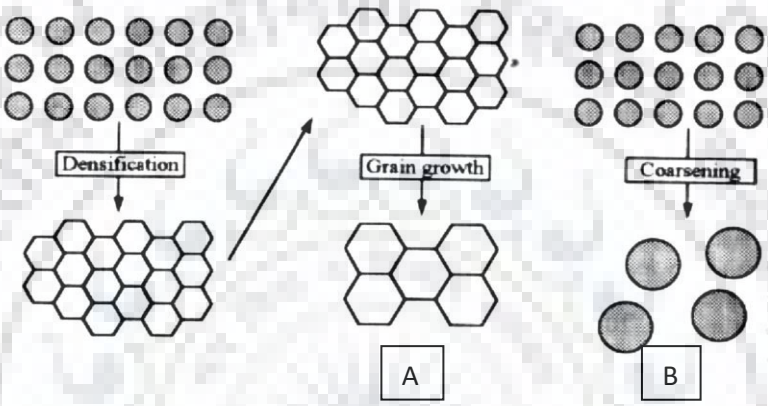

Fig11 (A) Schematic showing a typical densification phenomenon. (B) Schematic showing coarsening phenomenon

The two important points have come to light from various sintering mechanism proposed:

i. Mechanism responsible for coarsening is surface-diffusion which is prevalent at lower temperatures.
ii. Extended holding times at elevated temperatures are unable to restrict grain-growth.

These two problems can be solved if we are able to use a method which has high heating rates plus lower holding time at lower temperature.

This problems could be solved by using hot isostatic pressing sintering (HIP) as it has an inherent advantage over conventional process that is uses both pressure and temperature at the

same time. Pressure helps in bringing particles closer, thus helps in augmenting the mass transfer rate. Pressure application contributes for the increased densification kinetics via

i. Reduced stress due to the presence of larger interagglomerate pores
ii. Breakage of agglomerates
iii. Pore shrinkage via plastic deformation of grains

But, still holding temperatures are high and process is time consuming too. And one more concern is that the pressure requirement increases with decrease in particle size. For instance, pressure requirement for ultrafine powder rises to 500MPa as compared to only ~5MPa in case of micrometer sized powder compact.

$(\sigma = -2\gamma/r)$ Eqn. (1)

σ Sintering stress

γ Surface tension

r Pore radius

So, it can be clearly seen from the formula that as particle size goes down, requirement of sintering stress shoots up and in case of ultrafine cermets such stresses become so high that they are impractical to achieve practically.

But, SPS don't require such high pressure because it uses a synergetic combination of electrical energy and mechanical pressure. It is also called as the activated sintering as it has an inherent advantage of physically activating the particles by removing the contamination layer on the surface such that bare surface with high surface energy can actively take part in sintering. SPS involves three major qualities which enables it to lower the severity of the sintering conditions:

i. Like HIP, it is a pressure assisted sintering.
ii. It involves physical activation of the particles.
iii. It mechanism is such that it provides local heating effect at surface of powder particles which helps in restricting the grain growth.

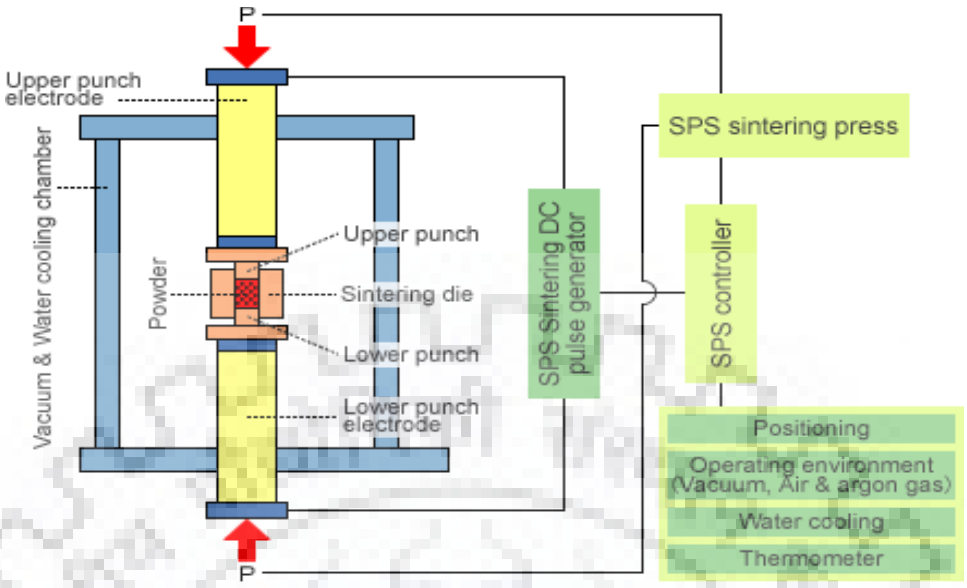

Fig. 12 Schematic diagram showing SPS setup[23]

Fig. 12 shows essential parts of a SPS machine which includes a die-punch assembly containing powder specimen is kept between two carbon electrodes of machine. These electrodes are linked to electric circuit which can provide pulsed current through specimen and also they are attached to a hydraulic system which can apply sintering pressure. The mechanism discussed here refers to ref. [23]. In SPS, initially there is spark discharge between powder particles by on-off pulse energization. This causes high temperature ionized gas column between particles called plasma which generates very high temperatures such that melting and vaporization takes place at particle surfaces. Then there is generation of spark impact pressure and sputtering. Sputtering mechanism generated by spark plasma and spark impact pressure removes adsorptive gases and impurities existing on the surface of the mixed powder particles. Sputtered melt connects adjacent particles and diffusion start taking place between particles by joule heating. With repeated application of On-Off DC pulse voltage these points of discharge and joule heating are transferred and dispersed uniformly through entire specimen. Further, heating and consequent diffusion takes place via joule heating only.

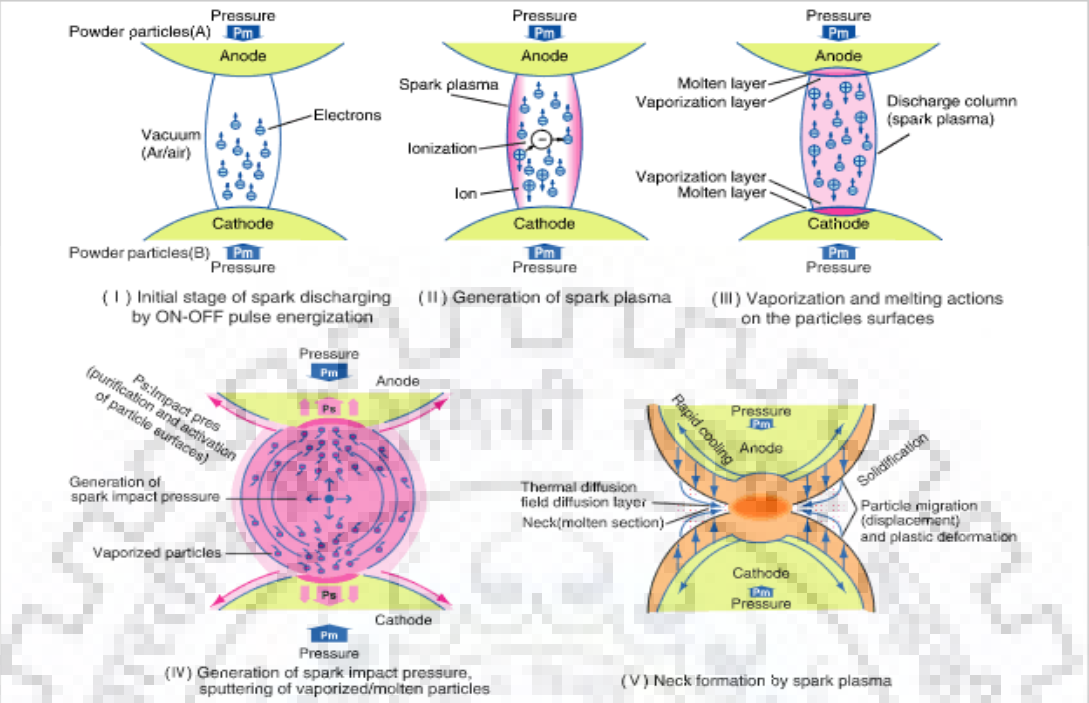

Fig.13 Schematic showing various stages in SPS process[24]

Various steps in SPS Mechanism:

Stage 1 There is a spark discharge between the charged particles.

Stage 2 Discharge ionizes the gas column between the powder particles, thus generating spark plasma.

Stage 3 Plasma leads to very high temperature generation at particle surfaces such that vaporization and melting takes place on particle surface.

Stage 4 Spark plasma leads to high pressure in between two powder particles that leads to spark impact pressure and sputtering of molten particles.

Stage 5 Sputtering reveals the virgin surfaces with high surface energy that leads to necking between powder particles.

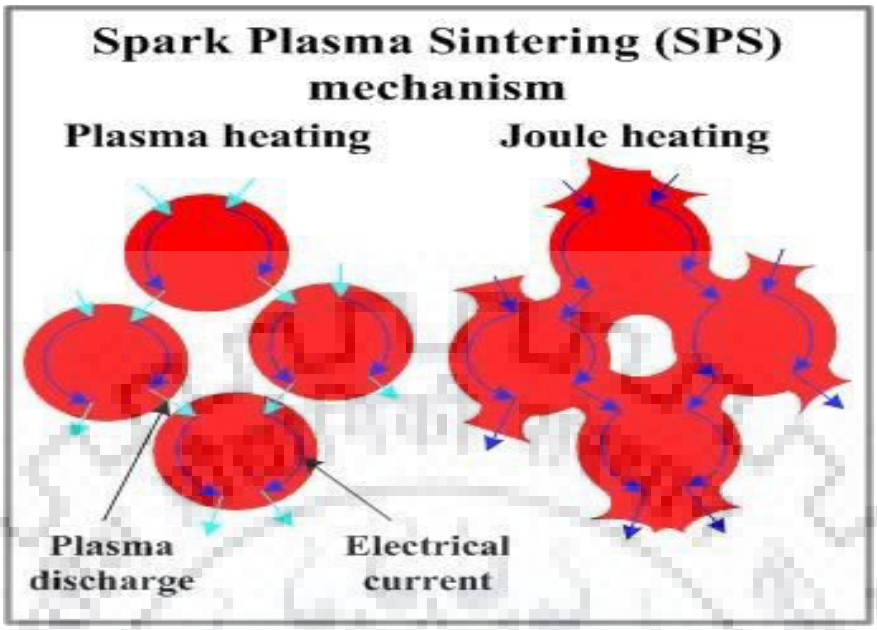

Fig. 14 Schematic diagram shows the joule heating between powder particles followed by initial plasma discharge.[25]

Various advantages of SPS are

i. Only particle surface is heated, so in absence of excess heat grain growth is prevented.
ii. Heat is supplied at a place where it is needed, so, low power consumption.
iii. Localized pulse causes enhanced diffusion, thus rapid sintering, thus preventing grain growth.
iv. SPS has 200°C less temperature than many of the conventional sintering and less holding times (maximum 10 min) . All these conditions prevent grain growth.

Despite of the advantages that SPS offers, it has some limitations also which includes limited shapes whish limits mass production, problem of leakage, porosity of as sintered cermets etc

In this chapter, experimental procedure involved in preparation, characterization and wear testing of sintered B_4C ceramic has been explained. The chapter has been divided into six sections including preparation of materials, milling of the powders, spark plasma sintering, density measurement, hardness measurement and dry sliding wear testing.

3.1. Preparation of the materials

As received SiC powder has an average particle size is on microns and BN .The sintering aid chosen for these powder was Yttrium Oxide (Y_2O_3) powder. The Y_2O_3 powder has an average particle size of 1 μm. The alumina powder has a purity of 99.9%. The X-ray diffraction analysis is carried out for the material characterization and to found different impurities and stoichiometries present in the powders.

3.2. Milling of the powders

The SiC-hBN(0,5,10,35wt%) power mixtures were milled in a jar mill in a bottle containing tungsten carbide balls of 10 mm diameter and filled with toluene for 24 hours. The weight of the balls to the weight of the powder mixture to be milled is maintained in the ratio of 10:1. The powders were then dried in oven at temperatures of about 120^{o}C with 3 hours duration and then sieved through a 45 μm sieve.

3.3. Spark plasma sintering

The sintering technique used in current work is spark plasma sintering (SPS-625,Fuji Electronics Ltd., Japan). The controlled SPS parameters are temperature, load applied and time of sintering. The powder was compacted in a graphite die to form a specimen of 10mm in diameter and 4mm in thickness. The heating rate was 100^{o}C/min. holding time was 5 min. maximum temperature 1800 ^{o}C, pressure was 55MPa and cooling rate was 200 ^{o}C/min.

Fig.15 Spark plasma sintering Facility

3.4. Density calculation method

The theoretical density of powder mixture was measured using the rule of mixtures as

$1/\rho = w1/d1 + w2/d2 + w3/d3$

where ρ is the theoretical density of composite.

w_1 weight fraction of first component.

d_1 density of first component.

The experimental density is calculated by water immersion method based on Archimedes principle. The sample weight both in air and water is measured and the experimental density i.e, density of sintered sample is calculated using the formula stated as

$Density_{experimental}$ = (weight of sample in air)/ (weight of sample in air – weight of sample in water)

The relative density is simply the ratio of experimental density to the theoretical density.

Relative density = $Density_{experimental}$/ $Density_{theoretical}$

3.5. Hardness and fracture toughness measurement

The hardness and fracture toughness of the polished samples were measured by Vickers indentation. For hardness measurement, the load applied was 0.5 kgf or 4.9N with a dwell time of 15 s which caused a diamond shape indentation on the samples. Both diagonals of indentation were identified and calculated using SEM images of the indentation and hardness is calculated using the Vickers indentation equation

$$\mathbf{H_v = 1.854(P/d^2)} \qquad \text{Eqn. (2)}$$

where H_v corresponds to Vicker's hardness test (in Pascal), P corresponds to applied load (in Newton), and d is average diagonal value of indenter (in metres).The indentation load should result to well developed as well as stable indentation without damage or cracking around indentation.

For fracture toughness a load of 3 kgf was applied for 15 s and the length of the cracks generated at the edges of Vickers indentation diagonals was measured. The fracture toughness (K_{IC}) was determined using Anstis formula (ref)

$$\mathbf{K_{IC} = 0.016\ (E/H)^{0.5}\ P/C^{1.5}} \qquad \text{Eqn. (3)}$$

An elastic modulus (E) of 410 GPa for SiC and 180 GPa for BN were considered for determining the elastic modulus of the SiC-BN composite by the rule of mixture.

3.6. Dry Sliding Wear Testing

The wear and friction behaviors of the composites were studied against SiC balls using a ball-on-disk (TR 201E-M2,DUCOM, India) (Fig. 3.5). Provided by manufacturer's description SiC is 28 GPa respectively. Before sliding wear testing, the composites and all the balls were cleaned ultrasonically using acetone, then dried in hot air stream.

The SiC ball was not moving it should be steady when the disk was rotated (500 rpm)and its linear speed was 0.157 m/s) to make a track diameter of 3 mm. The schematic diagram of sliding wear arrangement is shown in the Fig.16 Tests were done in ambient conditions (27 ± 5^0C and 30± 5% RH) at a single load of 10 N.

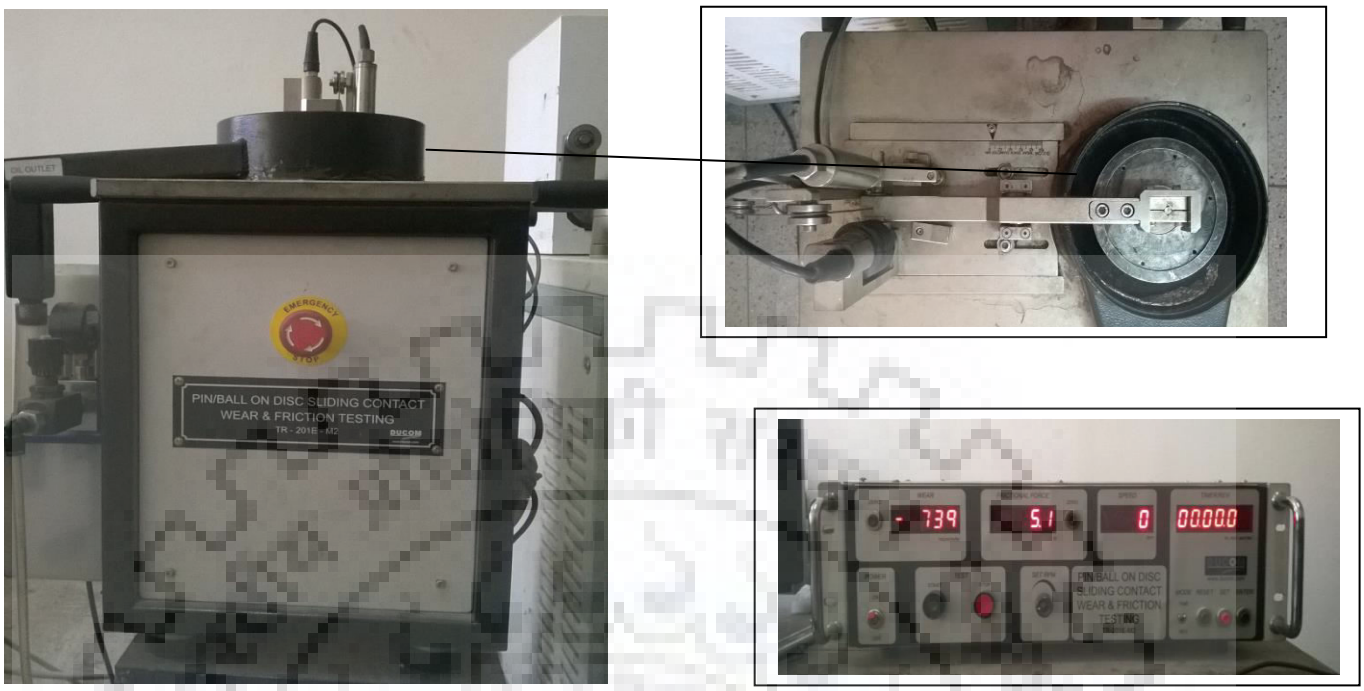

Fig.16 Ball on disk sliding wear facility

The frictional force was recorded time to time by electronic sensor to obtained a real time coefficient of friction (COF). The surface profiles of worn disk samples were analyzed to determine depth and width of worn surfaces using a profilometer (SJ 400, Mitutoyo, Japan). A minimum of 10 orthogonal measurements per track and only three tracks for each sample were studied to find the average values of depth as well as width of wearvscars. Values of depth as well as width were used for calculating volumetric wear damage. (V in mm^3).

$V = 2rwd$

where, r, w and d arevradius, width and depth of wear track, respectively (mm).

4.1 Characterization of received powders

The material characterization of as received silicon carbide (SiC) and boron nitride (BN) powders was carried out using the X-ray Diffraction technique. XRD was done for the conformation that the received powder has not any other major impurities.

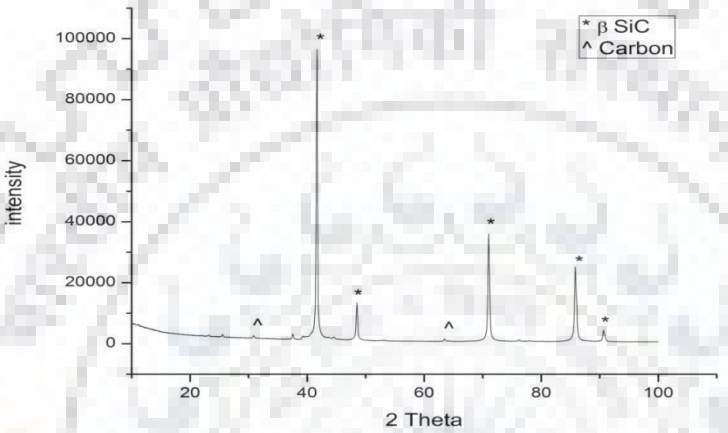

Fig.17 XRD analysis of as received SiC powder.

Fig. shows the XRD patterns for BN powder. From the XRD analysis of Boron Nitride, it was found that there are major peaks of hexagonal Boron Nitride.

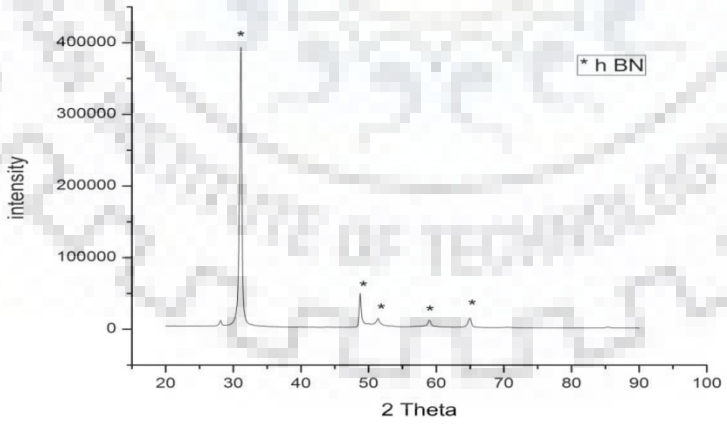

Fig.18 XRD analysis of as received BN powder

SEM analysis of powders indicated the size of powders is on microns and the elements presents are same as received powders that is for confirmation.

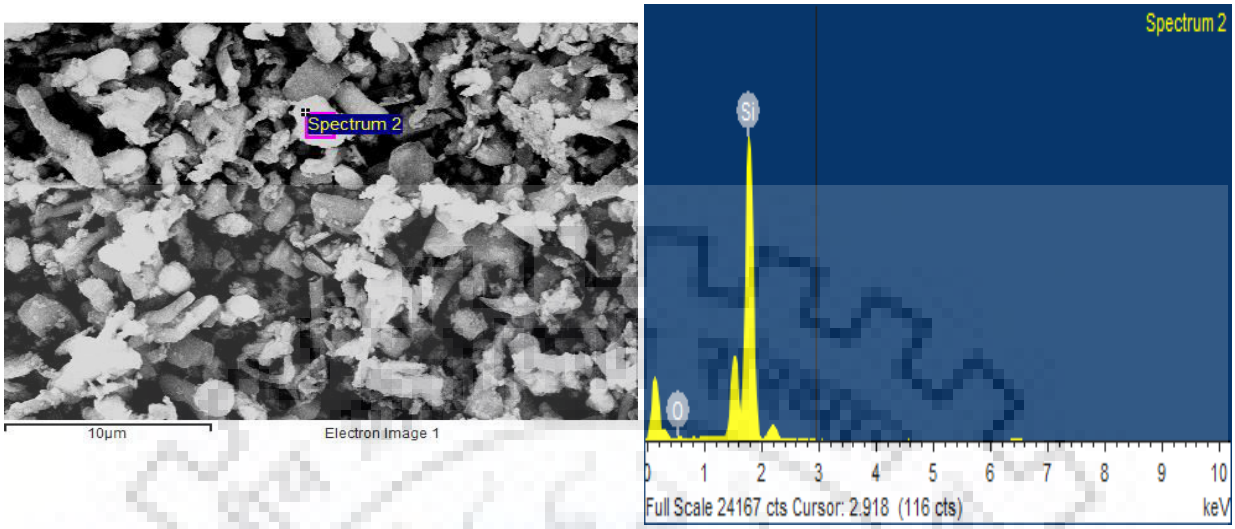

Fig.19 EDX analysis of SiC

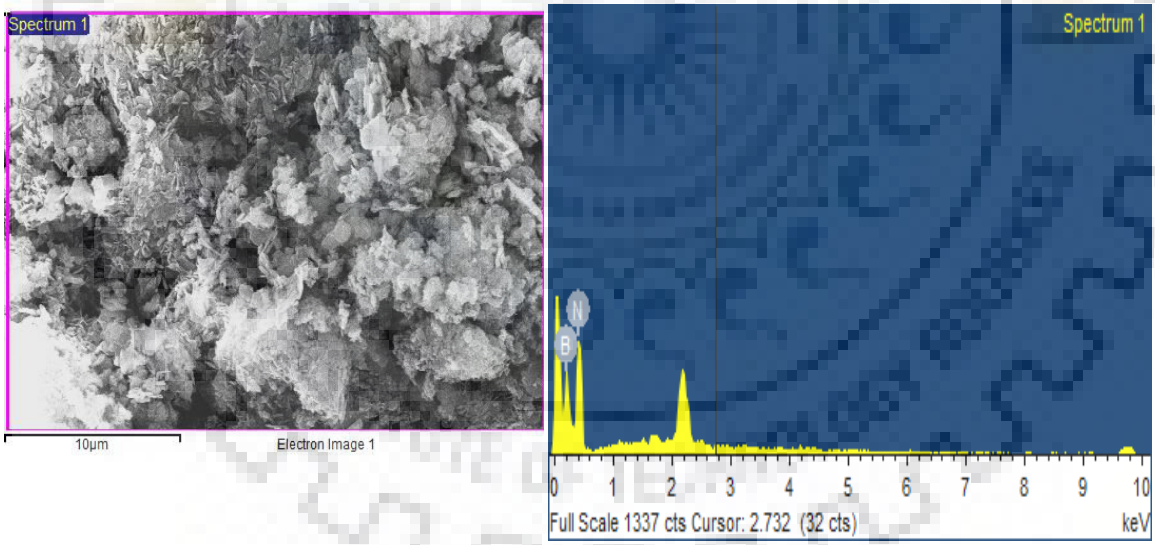

Fig20 EDX Analysis of BN

4.2 Density Calculation

The density of sintered sample was calculated using Archimedes principle.

$Density_{exp.}$ = (weight of sample in air)/ (weight of sample in air – weight of sample in water).

Table 3 Shows the Relative Density of the different composites

Composition	Relative Density %
SBN0	90.41
SBN5	96.08
SBN10	98.27
SBN35	98.32
SBN10 Without additive(Y_2O_3)	95.82

4.3 Microstructural characterization of composites

The relative densities of β SiC and SiC-BN composites are shown in Table 3. All specimens prepared using 2 vol.% Y_2O_3 as a sintering additive (except SBN10) showed relative density even greater than 99% after Spark Plasma sintering1800 ˚ C under applied pressure 55MPa in a argon atmosphere. Relative density of the composite with 35 vol.% BN (98.3%) was higher than the other specimens because of the impingement of BN grains in composites, resulted in the specimen and this leads to a limited densification. During sintering Y_2 O_3 reacts with the native Silicon oxide and B_2O_3, they are present on the surface of Silicon cardide and BN particles, respectively, to form a Yttrium boro silicate oxide melt. Again heating at high temperatures led to the formation of a Y-B-Si-OCN melt by diffusion of SiC, BN, and argon comes by the sintering atmosphere.Y-B-Si-OCN melt was responsible for the densification of the β SiC and SiC-BN composites via liquid phase sintering (18).

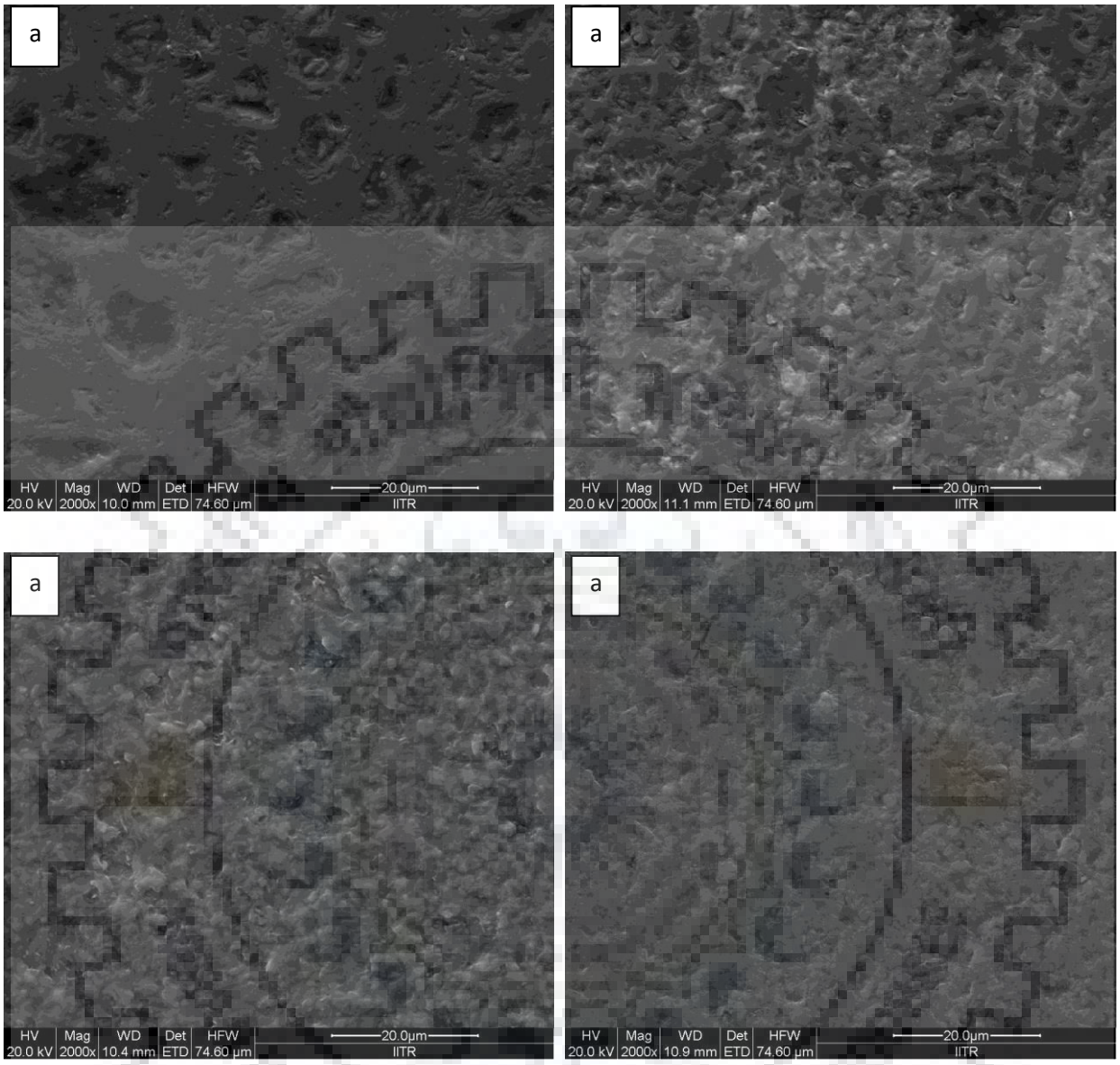

Fig.21 SEM images of SiC ceramics with (a) 5vol. % BN with additive (b) 10vol. % BN with additive (c) 35vol. % BN with additive (d) 10vol. % BN without additive

4.4 XRD analysis of composites

XRD patterns of composites sintered with Y_2O_3 were compared with that of β SiC ceramic sintered with Y_2O_3. No such peaks of Y_2O_3 attributed to the small amount (2 vol. %) of additive in the compositions. The β SiC was composed of SiC, whereas the SiC composites consisted of SiC, hexagonal BN, and Silicon carbide. By adding boron helps to stabilize the hexagonal structure of the SiC, whereas the addition of additive and oxynitride or OCN helps to stabilize

the cubic structure. Therefore, the $\beta \rightarrow \alpha$ phase transformation observed in the SiC-BN composites in literature which result of the competition among three materials: boron, nitrogen, and yttria. It is well documented that inter-diffusion of the B and N atoms occurred at the SiC/BN iinterface (18). As the BN-derived B and N atoms diffused into the SiC lattice at the SiC/BN interface.

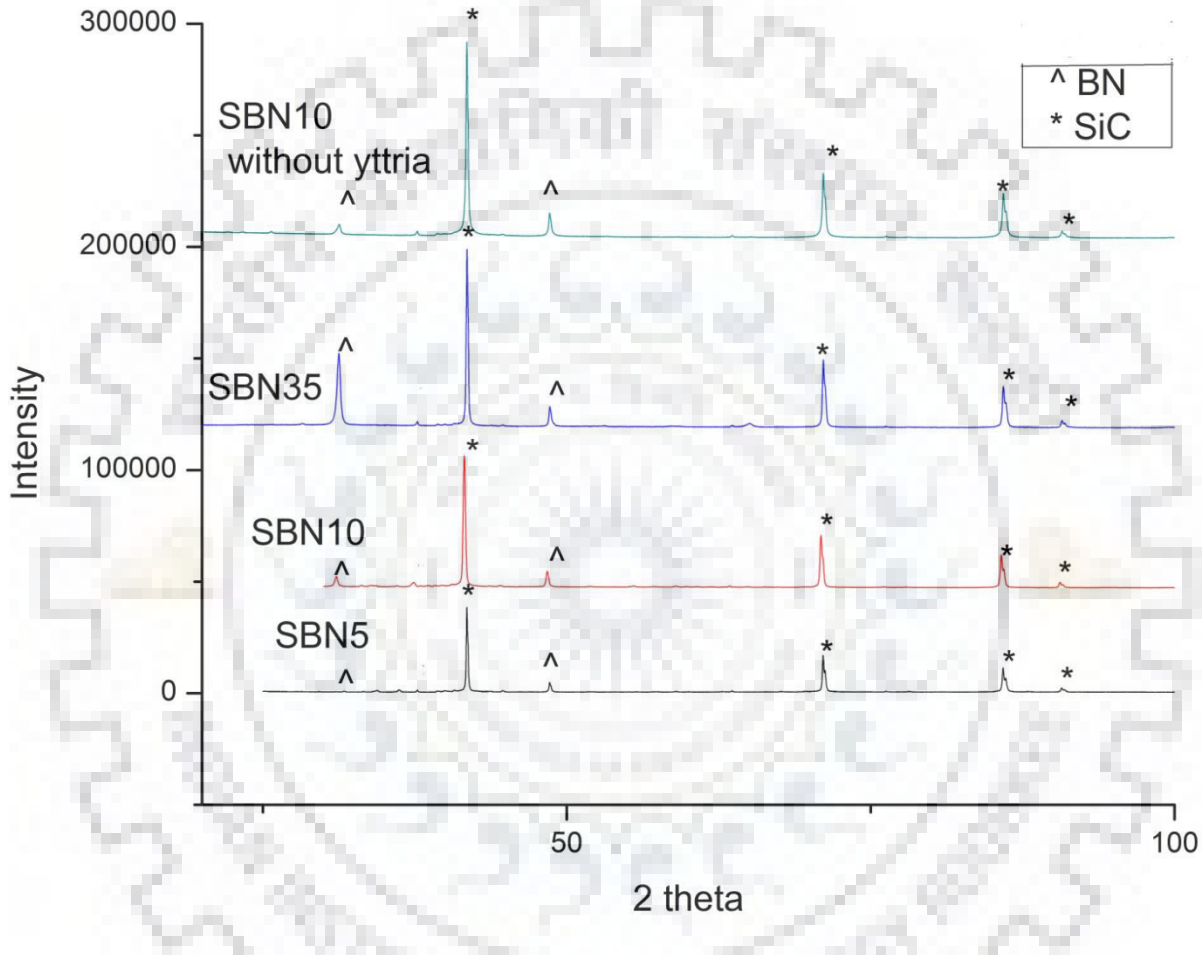

Fig.22 XRD analysis of the SiC-BN composites with different BN content

4.4 Mechanical Properties

The estimated values of hardness and fracture toughness listed in the Table 4. The value of the hardness is decreased with increasing BN content. The highest value of hardness is 19.20 GPa for SBN10 without additive and lowest value is 15.67 GPa for SBN10. Hardness and fracture toughness of the composites shown in Table 4.

Table4 Hardness and fracture toughness of the composites

Sample	**Hardness (GPa)**	**Fracture Toughness(Mpa-m$^{1/2}$)**
SBN5	19.20±0.4	2.33±0.2
SBN10	15.67±0.2	2.70±0.1
SBN35	16.73±0.3	3.93±0.2
SBN10 without Y_2O_3	17.86±0.4	2.50±0.1

4.4 Sliding wear of composites

4.4.1 Frictional behavior

The unlubricated sliding wear test subjected against SiC ball with 10N load for 45 minutes at 500 rpm to all composites. The value of coefficient of friction is between 0.26-0.43 (see Fig.23). As the BN content is increased 5 to 10 vol. % the COF is decreased but for 35 vol.% it increased to 0.26 to 0.35 and in comparison to without additive COF is also increased.

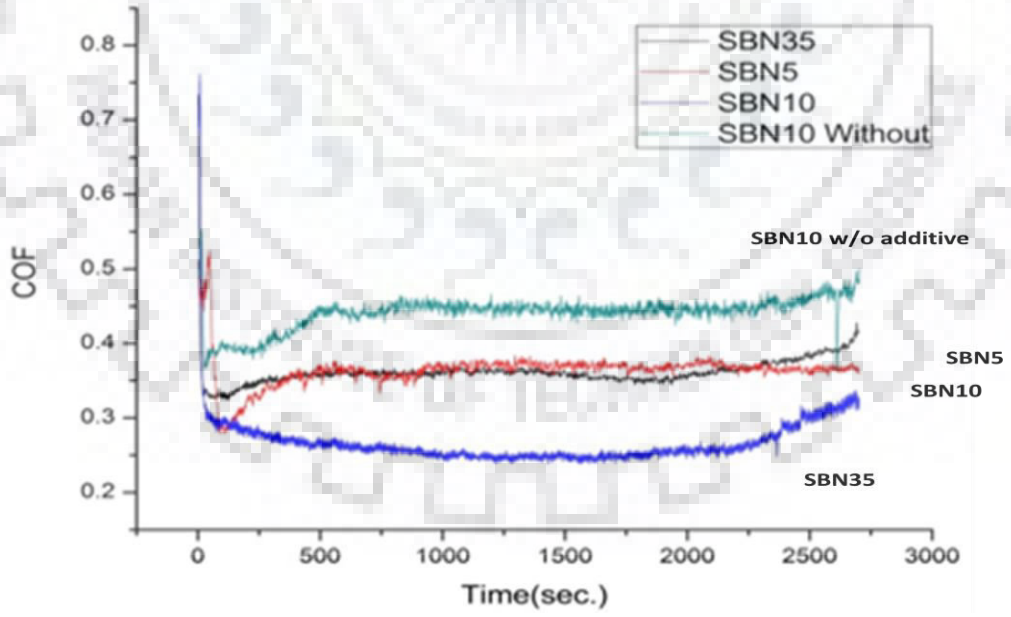

Fig23 Coefficient of friction vs time for the investigated composites.

4.4.2 Wear Results

Typical surface profiles of the wear scar acquired in the perpendicular direction of sliding are shown in Figure 24 and calculated wear volume of composites is shown in fig.

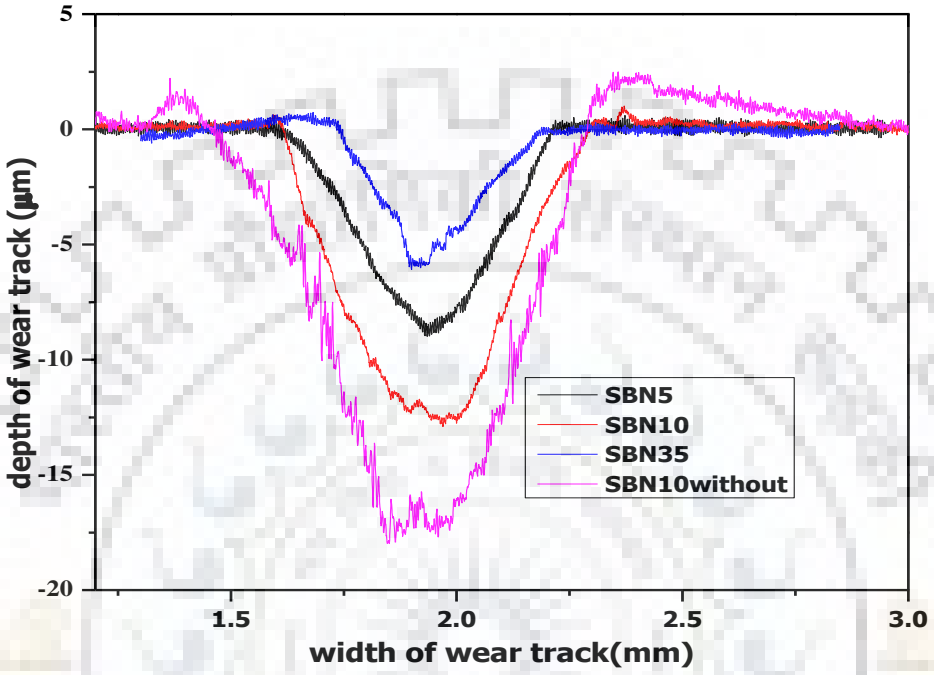

Fig.24 Depth of wear track vs width of wear track for the investigated composites.

From fig.24 it is observed that wear track width and wear track depth decreased from SBN5 to SBN35. Wear track width and wear track depth of SBN10 without Y_2O_3 is found maximum.From fig.25 Wear volume calculated of wear track decreased from 4.8 x 10^{-2} mm^3 to 6.4 x 10^{-3} $mm^3$for SBN5 to SBN35 respectively. Maximum wear volume of 6.8 x 10^{-2} mm^3 was found in case of SBN10 without Y_2O_3. Therefore SBN35 showed maximum wear resistance and SBN10 without Y_2O_3 showed least wear resistance. 1 order of difference in wear volume was found SBN35 to SBN10 without Y_2O_3.

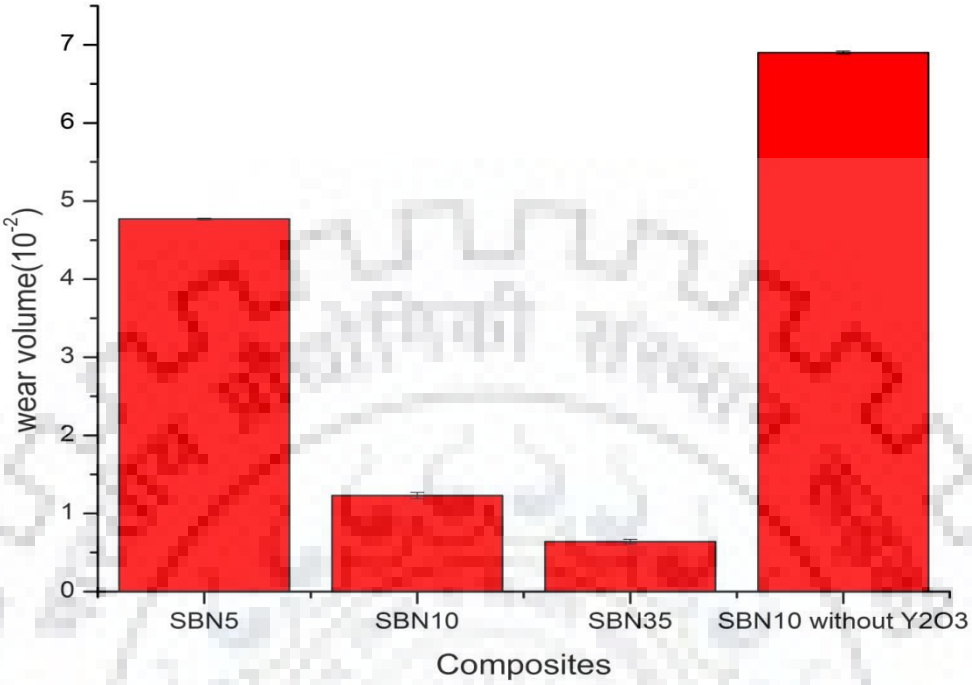

Fig25 Shows the bar graph of wear volume of different composites

4.4.3 Worn Surface Analysis

Worn Surface of SiC-BN composites were analyzed by SEM analysis to find mechanisms of material removal in this conditions of the sliding. The severity of sliding damage significantly decreased as the BN content increased from 5 to 35 vol.%, during sliding for longer duration of 45 min with sliding speed of 0.1 m/sec. SEM images of composites are shown in Fig. at low magnification. From fig.26 observed that width of the wear scar decreased with increase in BN content. For example, width of the scar decreased from 506µm to 268 µm as BN content is increased.

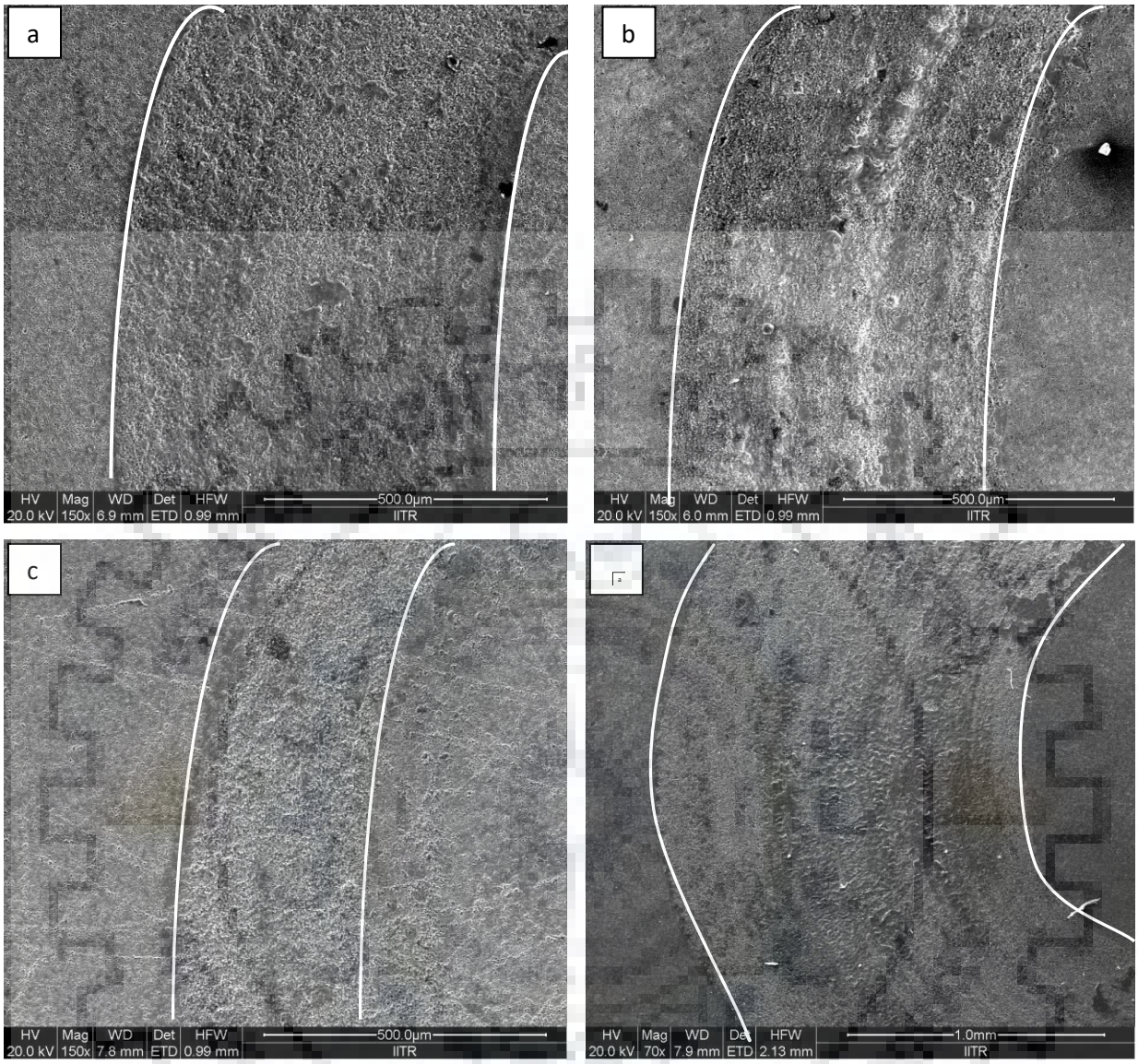

Fig. 26 SEM images of worn surfaces of composites (a)5 vol. %BN with additive (b)10 vol. %BN with additive (c)35 vol. %BN with additive (d)10 vol. %BN without additive

The least wear scar width (268 µm) is observed for SBN35 and maximum wear scar width (1300 µm) was observed for SBN10 without additive. From fig, maximum severity of wear is observed in SBN10 without additive and minimum severity of wear was observed in SBN35. As we go to the higher magnification (5000X) for the wear surface the severity of the wear is clearly visible and also the fracture surface. As the BN content is increasing the wear volume is decreasing which is clearly shown below in given figures. To find out possible wear mechanism responsible for wear, higher magnification SEM images of worn surface of composites are shown in Fig.26

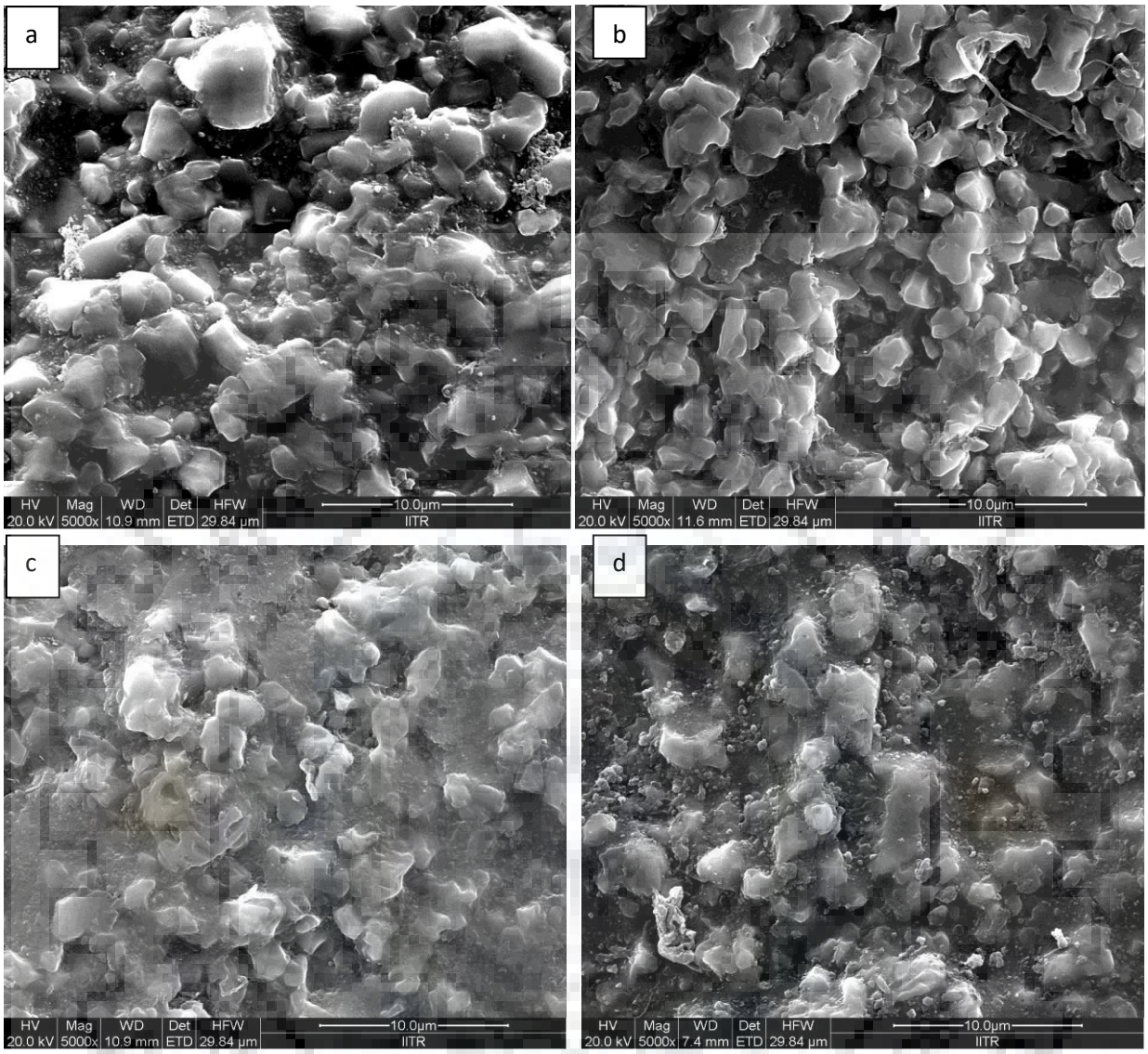

Fig27 SEM images of the wear track (a)5 vol. %BN with additive (b)10vol. %BN with additive (c)35vol. %BN with additive (d)10 vol. %BN without additive

Mainly mechanical fracture of and particles pull-out were observed from Fig27.which are responsible for wear of composites. Particles pull-out were reduced with the increase in BN content from 5 vol% to 35 vol% SBN35 vol% showed high wear resistance due to have layer structure with mechanical fracture. This layer structure reduces the mechanical fracture and pullout of BN particles which is weaker phase in matrix. SBN10 vol. %BN without additive showed least sliding resistance against SiC counterbody due to high pull-out of weaker phase and severe mechanical fracture. Microstructure of fracture surface of composites is shown in

Fig. The wear characteristics can be explained from the fractured microstructures. From Fig.28 It is clear visible that SBN35 has less pull out and mechanical fracture than SBN5 due to have layer structure. In fig b and d, The additive effect of Y2O3 is observed because the presence of Y2O3 in SBN10 allows mechanical fracture of grains while tearing of grains with severe mechanical fracture were observed in fig d..

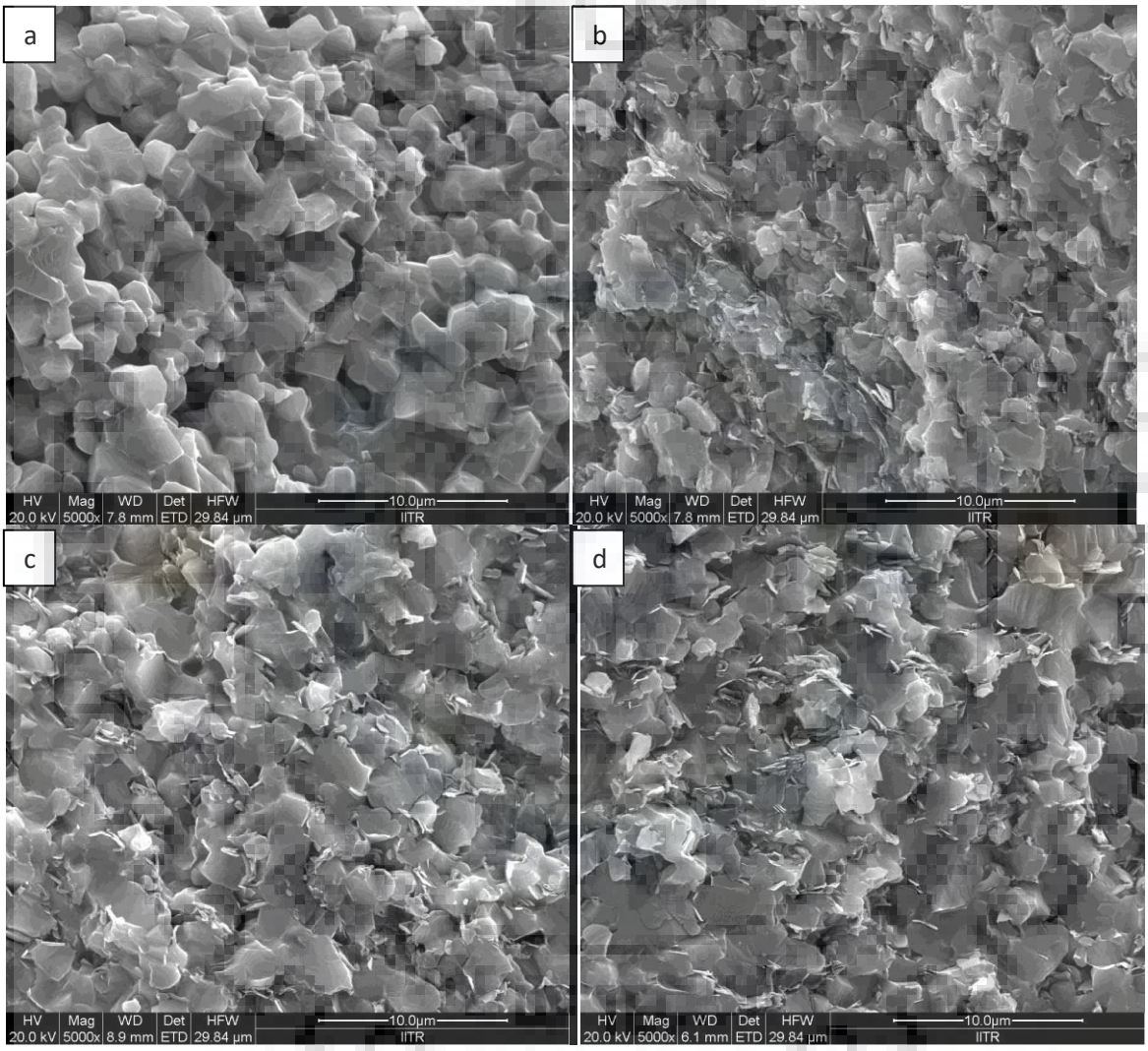

Fig.28 SEM images of the fractured surface (a)5vol.%BN with additive (b)10vol.%BN with additive (c)35vol.%BN with additive (d)10vol.%BN with additive

4.4.4 Wear analysis of debris and balls

When the ceramics slides each other, mechanical processes like indentation, abrasion, and fracture produce a lots of debris particles contact area is increased by several order of magnitude.

In order to understand the relationship between characteristics of debris and tribological performance of these debris is analyzed SiC ceramics, debris particles comes from worn SiC ceramics surfaces were collected very carefully and analyzed by SEM.

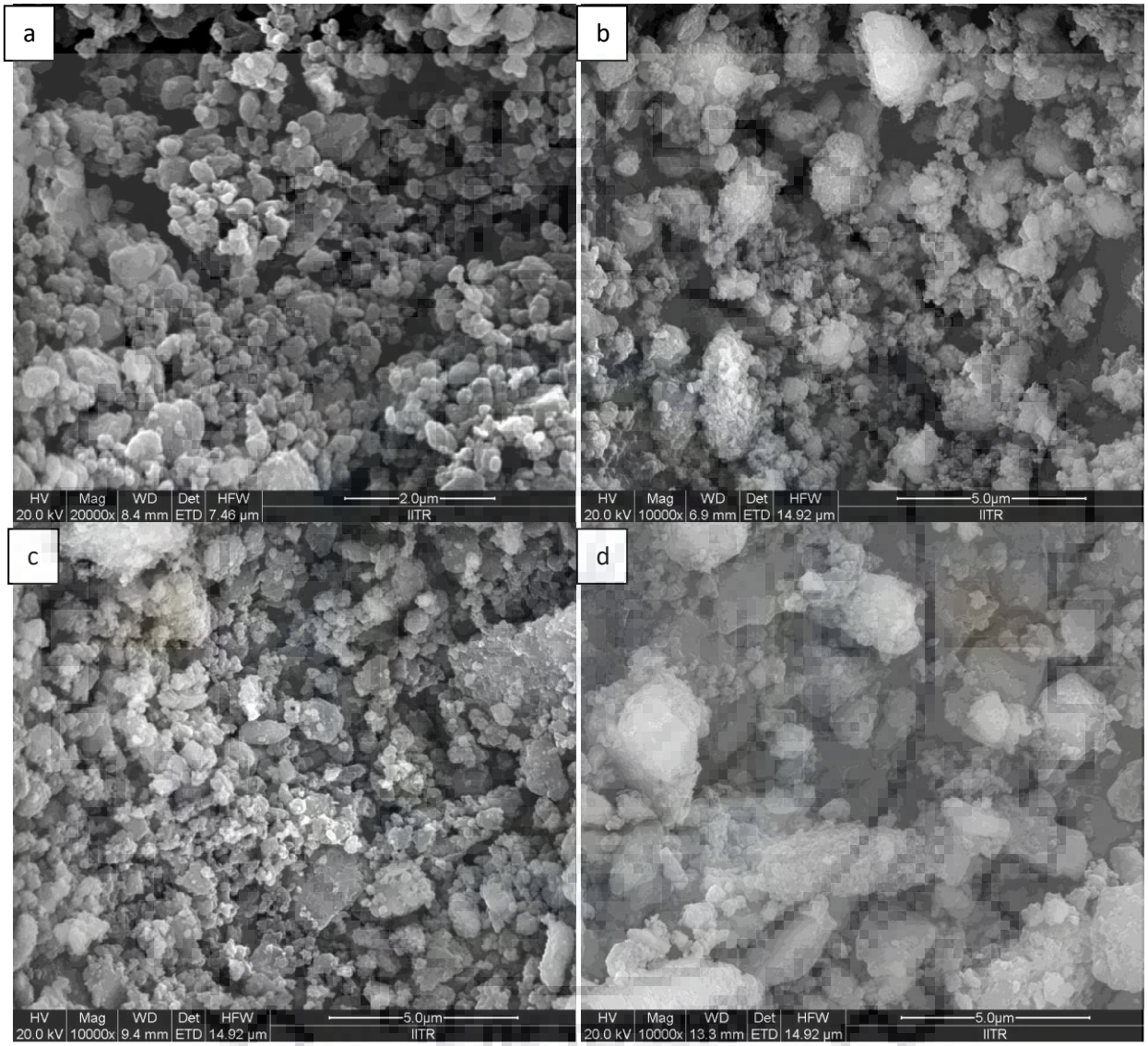

Fig.29 SEM images of the wear debris (a)5vol.%BN with additive (b)10vol.%BN with additive (c)35vol.%BN with additive (d)10vol.%BN with additive

From the fig.28 the particle size of the wear debris is decreased as the BN content is increased which is also explained as from the fracture toughness is increased and hardness is decreased, from fig.28(d) i.e BN10 without additive which has hardness more than SBN10 or SBN35 shows more wear debris also it is non uniform than all others compositions.

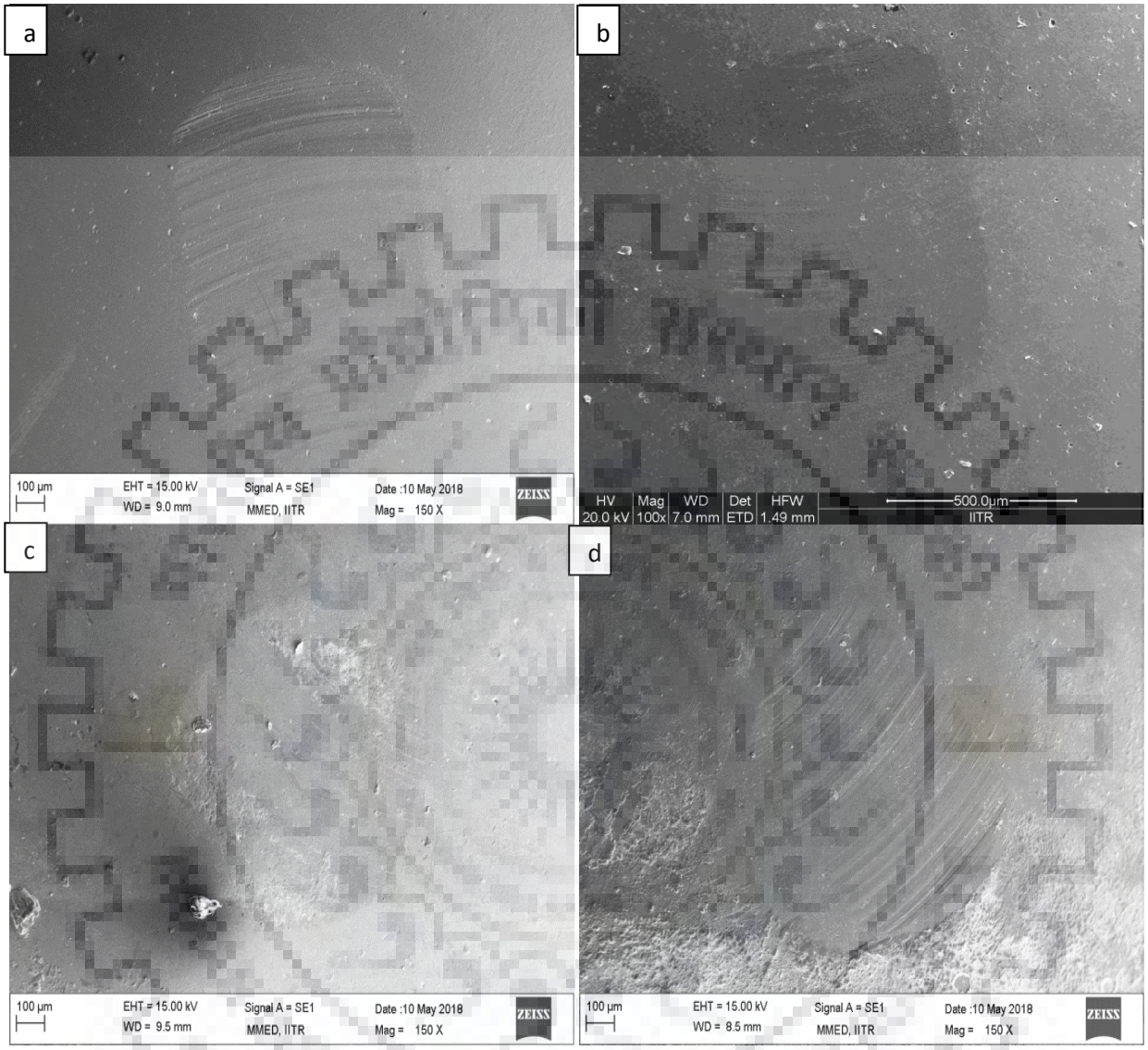

Fig.30 SEM images of the wear debris (a)5vol.%BN with additive (b)10vol.%BN with additive (c)35vol.%BN with additive (d)10vol.%BN with additive

The shape of wear scar on ball is almost oval on all counter body of respective composites except SBN10 without Y2O3. Because in case of SBN10 without Y2O3 wear scar changes from circular to oval shape. Counter body of SBN35 composites has mild abrasion with transfer of tribo layer while other counter body of respective composites has abrasion on surface Counter

body of SBN35 shows least wear in size and SBN10 without Y2O3 shows severe wear of counter body which are completely in the relevance with worn surface of composite.

SiC-BN composites 0 vol.%, 5 vol% , 10 vol% and 35 vol.%BN contents ceramics formed by spark plasma sintering at 1800C for 5min , at 55 MPa. The effect of BN addition was investigated for microstructural, mechanical properties of sintered composites. The behaviour of sintered composites during dry sliding was investigated. The following are major conclusions:

a) The density of sintered composites increased with increase in BN content. High density with good bonding between SiC and BN grains comes at 35vol% BN composite with the optimum SPS conditions.

b) Hardness, fracture toughness is increased with BN content A combination of high microhardness ($19.20 \pm \mathbf{0.4}$GPa), high fracture toughness ($3.93 \pm \mathbf{0.2}$MPa.$m^{1/2}$) obtained for SiC-35vol% BN composite. Mixture fracture of BN grains, tearing and grain pull out of SiC particles are observed for all SiC –BN composites.

c) Dry sliding wear against SiC balls at 10 N load for 45 min. is done for all composites. From wear analysis we get the severity of wear is maximum at SBN5 than it goes on decreased at BN content increased among all max. at SBN10 with additive Y_2O_3 and mechanical fracture, pull-out ant transgranular fracture are observed that is maximum at SBN35 which is mixed type, for SBN10 with additive and without additive additive addition resist the fracture.

Chapter6 Scope of Future work

In the present work, same load , BN content, counterbody on tribological behaviour are understood in unlubricated sliding wear conditions, while the study can be extended for the effect of different loads, different counter bodies and also at different temperatures other parameters like etc:

[1] Similarly, effect of test parameters and materials (BN content) on friction and wear properties in sliding wear with lubrication can be studied.

[2] The erosion wear can be further studied to understand the effect of velocity of particle impingement and type of erodent particles in high temperature erosion conditions.

[3] The potential of the newly developed SiC-BN composites can be further assessed by the studying the behaviour in other wear modes like cavitation, fretting etc.

[1] W.B. Hillig, Ceramics for High Performance Applications, Vol. 2, edited by J.J. Burke, E.N. Lenve, and R.N. Katz, Brook Hill Publishing Company, Chestnut Hill, Maryland, 1978, pg. 989.

[2] R.L. Mehan, G.G. Trantina, C.R. Morelock, "Properties of a Compliant Ceramic Layer," Journal of Materials Science, Vol. 16, 1981, pp. 1131-1134.

[3] L.D. Bentsen, D.P.H. Hasselman, and R. Ruh, "Thermal Diffusivity of SiC-BN Composites," Basic Science Division, Fall Meeting of The American Ceramic Society, 31 October 1983, Columbus, Ohio, No. 17-B-83F.

[4] D.P.H. Hasselman, P.F. Becher, and K.S. Mazdiyasni, "Analysis of the Resistance of High-E, Low-E Brittle Composites to Failure by Thermal Shock," Z. Werkstoff Tech., Vol. 11, 1980, pp. 82-92.

[5] D.P.H. Hasselman and P.T.B. Shaffer, WADD-TR-60-749, Part II,1962.

[6] R.C. Rossi, Ceramics in Severe Environments, edited by W.W. Kriegel and H. Palmour III, Plenum Press, New York, 1971, pp. 123- 136.

[7] K.S. Mazdiyasni and R. Ruh, "High/Low Modulus Si *3N* -BN Composite for Improved Electrical and Thermal Shock Behavior," Journal of The American Ceramic Society, Vol. 64, No. 7 , July 1981, pp. 415-419.

[8] D.J. Godfrey, "The Use of Ceramics in Engines," Proceedings of the British Ceramic Society, Vol. 26, July 1978, pp. 1-15.

[9] Jin Z.J., Zhang M., Guo D. M.and Kang R. K., Electroforming of copper/ZrB_2 composite coating and its performance as electro-discharge machining electrodes., Key. Eng. Mater., 2005, 291–292, 537–42.

[10] Sung J., Goedde D. M., Girolami G. S. and Abelson J. R., Remote-plasma chemical vapor deposition of conformal ZrB_2 films at low temperature: a promising diffusion barrier for ultralarge scale integrated electronics., J, Appl, Phys,, 2002, 91(6), 3904–11.

[11] Murata Y., Cutting tool tips and ceramics containing hafnium nitride and zirconium diboride., U.S. Patent No. 3, 1970, 487, 594,.

[12] Tripp W. C., Davis H. H. and Graham H. C., Effect of a silicon carbide addition on the oxidation of zirconium diboride., Am. Ceram. Bull., 1973, 52(8), 612–616.

[13] Fahrenholtz W. G., Hilmas G. E., Chamberlain A. L. and Zimmermann J. W., Processing and characterization of ZrB_2-based ultra-high temperature monolithic and fibrous monolithic ceramics., J. Mater. Sci., 2004, 39(19), 5951–5957.

[14] Monteverde F. and Bellosi A., Oxidation of ZrB_2-based ceramics in dry air., J. Electrochem. Soc., 2003, 150(11), B552–B559.

[15] Pastor M., Metallic borides: preparation of solid bodies, sintering methods and properties of solid bodies. InBoron and Refractory Borides, ed. V. I. Matkovich. Springer, New York., 1977, 457–493.

[16] Meeson G. A. and Gorbunow A. F., Activated sintering of zirconium boride., Inorg. Mater., 1968,4, 267–270.

[17] Kinoshita M., Kose S. and Hamano Y., Hot-pressing of zirconium diboride-molybdenum disilicide mixtures., Yogyo-Kyokai-Shi, 1970, 78(2), 32–41.

[18] Guo S. Q., Yang J.-M., Tanaka H. and Kagawa Y., Effect of thermal exposure on strength of ZrB_2-based composites with nano-sized SiC particles., Comp. Sci. Technol., 2008, 68(14), 3033–3040.

[19] Kalish D. and Clougherty E. V., Densification mechanisms in high-pressure hot-pressing of HfB_2., J. Am. Ceram. Soc., 1969, 52(1), 26–30.

[20] Kalish D., Clougherty E. V. and Kreder, K., Strength, fracture mode and thermal stress resistance of HfB_2 and ZrB_2., J. Am. Ceram. Soc., 1969, 52(1), 30–36.

[21] Monteverde F. and Bellosi A., Development and characterization of metal diboride-based composites toughened with ultra-fine SiC particulates., Solid State Sci., 2005, 7, 622–630.

[22] Monteverde F., Beneficial effects of an ultra-fine SiC incorporation on the sinterability and mechanical properties of ZrB_2., Appl. Phys. A: Mater. Sci. Eng., 2006, 82(2), 329–337.

[23] Zhang S. C., Hilmas G. E., and Fahrenholtz W. G., Pressureless Sintering of ZrB_2–SiC Ceramics., J. Am. Ceram. Soc., 2007, 91(1), 26–32.

[24] Y. Yan, H. Zhang, Z. Huang, J. Liu, and D. Jiang, In Situ Synthesis of Ultrafine ZrB_2-SiC Composite Powders and the Pressureless Sintering Behaviors., J. Am. Ceram. Soc., 2008, 91(4), 1372–6.

[25] Zhang H., Yan Y., Huang Z., Liu X., and Jiang D., Pressureless Sintering of ZrB_2–SiC Ceramics: The Effect of B_4C Content., Scr. Mater., 2008, 60(7), 559–62.

[26] Rezaie A., Fahrenholtz W. G., and Hilmas G. E., Effect of Hot Pressing Time and Temperature on the Microstructure and Mechanical Properties of ZrB_2–SiC., J. Mat. Sci., 2007, 42(8), 2735–44.

[27] Zimmermann J. W., Hilmas G. E., Fahrenholtz W. G., Monteverde F. and Bellosi A., Fabrication and Properties of Reactively Hot Pressed ZrB_2–SiC Ceramics., J. Euro. Ceram. Soc., 2007, 27(7) 2729–36.

[28] Monteverde F., Bellosi A. and Guicciardi S., Processing and Properties of Zirconium Diboride-Based Composites., J. Euro. Ceram. Soc., 2002, 22(3), 279– 88.

[29] Bellosi A., Monteverde F. and Sciti D., Fast Densification of UltraHigh-Temperature Ceramics by Spark Plasma Sintering., Int. J. App. Ceram. Tech., 2006, 3(1), 32–40.

[30] Guo S., Densification of ZrB_2-Based Composites and Their Mechanical and Physical Properties: A Review., J. Euro. Ceram. Soc., 2009, 29 (6), 995–1011.

[31] Wilson A., Hot Structures and Thermal Protection Systems for Space Vehicles in Proceedings of the 4th European Workshop, Palermo, Italy, 2002, 65.

[32] Tokida M., Trends in advanced spark plasma sintering system and technology.J. Soc. Powder Technol. Jpn., 1993, 30(11), 790–804.

[33] Nygren M. and Shen Z., On the preparation of bio-, nano- and structural ceramics and composites by spark plasma sintering., Solid State Sci., 2003, 5, 125–131.

[34] Medri V., Monteverde F., Balbo A. and Bellosi A., Comparison of ZrB_2–ZrC–SiC composites fabricated by spark plasma sintering and hotpressing., Adv. Eng. Sci., 2005,7, 159–163.

[35] Upadhya K., Yang J. M. and W. P. Hoffman W. P., Material for ultrahigh temperature structural applications., The Amer. Ceram. Soc. Bull., 1997, 76, 51.

[36] Ghosh D., Subhash G. and Bourne G. R., Inelastic deformation under indentation and scratch loads in a ZrB_2–SiC composite., J. Euro. Ceram. Soc., 2009, 29, 3053–3061.

[37] Clougherty E. V., Pober R. L. and Kaufman L., Synthesis of oxidation resistant metal diboride composites., Trans. Metall. Soc. AIME, 1968, 242, 1077.

[38] Bull J., In 19th Conference on Composite Materials and Structures CIAC, Cocoa Beach, FL, 1995, 157.

[39] Metacalfe A. G., Elsner N. B., Allen D. T., Wuchina E., Opeka M. and Opila E., High temperature corrosion and material chemistry., Electrochem. Soc. Proc., 1999, 99, (38), 489.

[40] Talmy I. G., Zaykoski J. A. and Opeka M. A., Properties of ceramics in the ZrB_2/ZrC/SiC system prepared by reactive sintering., Ceram. Eng. Sci. Proc., 1998, 19, 105.

[41] Marshall J., Erlich D. C., Manning H., Duppler W., Elliberby D. and Gasch M., Microhardness and high-velocity impact resistance of HfB_2/SiC and ZrB_2/SiC composites, J. Mater. Sci., 2004, 39, 5959 – 5968.